SSRG International Journal of Civil Engineering
ISSN: 2348-8352/ https://doi.org/10.14445/23488352/IJCE-V13I8P109

Volume 13 Issue 8, 152-171, August 2026
© 2026 Seventh Sense Research Group®

Original Article

Flexural Performance of Hollow-Core RCA T-Beams Strengthened with GFRP Sheets via EBROG Technique under Negative Moment

Sumeya Assim Hameed[1], Hasan Jasim Mohammed[1]

[1]*Department of Civil Engineering, Faculty of Engineering, Tikrit University, P.O. Box (42), Tikrit, Iraq*

[1]*Corresponding Author : ms.sumiyaassaim@tu.edu.iq*

Received: 17 February 2026 Revised: 25 March 2026 Accepted: 15 July 2026 Published: 31 August 2026

***Abstract* -** The construction industry is increasingly seeking sustainable solutions that do not compromise structural integrity. The present study evaluates the flexural performance of full-scale hollow-core Reinforced Concrete (RC) T-beams incorporating the Recycled Concrete Aggregate (RCA) with FRP strengthening using Glass Fiber Reinforced Polymer (GFRP) grids. The experimental work comprised six T-beams (3600 mm length) tested under three-point loading in an inverted configuration to simulate the negative moment region over supports. The tested specimens are divided into two groups based on replacement ratios of RCA and the application of strengthening. The replacement ratios were (0%, 50%, and 100%). To mitigate the premature debonding often associated with RCA surfaces, the Externally Bonded Reinforcement on Grooves (EBROG) technique was proposed. The findings revealed that replacing natural aggregates with RCA did not compromise the bearing capacity, remarkably, beams with higher RCA content exhibited an enhancement in concrete compressive strength of up to 16%. The application of GFRP strengthening further enhanced the bearing capacity by 7% compared to unstrengthen counterparts. All beams demonstrated ductile failure modes, with strengthened specimens failing primarily through GFRP rupture or partial debonding. These findings suggest that the EBROG technique effectively anchors GFRP to RCA concrete, making the combination of hollow-core geometry and recycled aggregates a viable, sustainable alternative for structural applications in negative moment regions.

Keywords - *Recycled Concrete Aggregate (RCA), EBROG, Hollow-core T-beam, GFRP strengthening, Negative moment.*

1. Introduction

A major concern has arisen in the last few decades about the planet's ecosystems. If no attentions given to the adverse environmental impacts, mineral deposits and raw materials will be lost of causing irreversible harm to the Earth's environment and atmosphere [1].

Ensuring the sustainability of the global construction industry is a significant challenge, with the sector consuming approximately (3000 times 10^6) tons of raw materials annually—double that of any other industry. Thousands of demolished concrete specimens are generated daily as a result of laboratory testing for new construction projects and research studies [2], and thousands tones of truck mixer wastes produced daily all-over the world. This massive consumption is paralleled by the generation of significant building and destruction waste, leading to environmental degradation and land encroachment. To address these challenges, the utilize of Recycled Concrete Aggregate (RCA) as an alternative to natural aggregates, either partially or completely, has gained significant attention. Many researchers studied the utilizing of crushed concrete as a coarse aggregate in a partial or complete replacement of natural aggregates in new construction.

However, the structural use of Recycled Concrete Aggregate (RCA) remains limited because of its inferior mechanical properties. Compared with natural aggregates, RCA generally exhibits lower strength and a reduced modulus of elasticity, primarily because of the porous stick to mortar on its surface and the existence of a weaker Interfacial Transition Zone (ITZ). RCA is characterized by higher water absorption and a more angular particle shape than natural aggregate, resulting in variations in the compressive strength of concrete. Consequently, RCA concrete is mainly used in road base applications and non-structural concrete elements. While various treatments—such as acid soaking, thermal treatment, or polymer impregnation—have been proposed to enhance RCA properties, they often incur high costs or logistical complexity.

Various techniques have been proposed to enhance the mechanical properties of concrete, including heating to different temperatures, pre-soaking in acid solutions of varying concentrations, and mechanical treatment using a Micro-Deval device with or without steel balls. [3]. A portion of the stick to mortar from RCA is mechanically removed utilizing a Los Angeles abrasion machine, together with acid pre-soaking and heating to 400°C, has been shown to improve the quality of RCA compared with untreated samples [4]. Addition of steel fiber has been reviewed and investigated by many authors as a beneficial method of treatment [5, 6]. Traditional treatment methods for Recycled Concrete Aggregate (RCA), such as acid pre-soaking and mechanical grinding, present several drawbacks. Acid treatment can increase processing costs, whereas mechanical grinding may induce micro-cracks that weaken the internal structure of the aggregate. Consequently, improving the quality of the adhered mortar layer has emerged as a more practical and economical approach. One commonly adopted technique involves coating the RCA surface with polymer emulsions, including Polyvinyl Alcohol (PVA) and silane-based polymers, which help decrease water absorption and enhance aggregate performance. Another effective method is the treatment of RCA with pozzolanic materials prior to its incorporation into concrete.

Pozzolanic additives, such as silica fume and fly ash enhance RCA characteristics through two primary mechanisms: they are filling the pores and micro-voids within the adhered mortar, thereby reducing water absorption, and they participate in pozzolanic reactions with calcium hydroxide to generate additional calcium silicate hydrate (C–S–H) gel, resulting in a denser microstructure and improved aggregate quality [7]. On the other hand, [8] stated that the incorporation of recycled CA as a replacement for normal aggregate had little to no effect on the compressive strength of concrete because both the Natural Aggregate (NA) and RCA were used in a Saturated Surface-Dry (SSD) condition. According to other researches, RCA concrete's compressive strength enhanced when the water-to-cement ratio was raised [1]. The incorporation of RCA as a substitute for natural aggregate have found to increase the concrete compressive strength associated by conventional mixtures, while having little to no influence on its flexural and splitting tensile strengths [9]. Several studies have examined the bending performance of RC beams produced with RCA. Most of previous studies have found that reinforced concrete beams incorporating RCA as a replacement for natural aggregate often have low performance compared to the conversional aggregate reinforced concrete beam. As for concrete made with RCA exhibited lower compressive strength, lower elasticity and tensile strength. Reinforced concrete beams incorporating Recycled Concrete Aggregate (RCA) exhibited closer flexural crack spacing, wider cracks, greater deflections, higher strain levels, and lower initial stiffness than beams made with natural aggregates, while their ultimate load-carrying capacity was either comparable or slightly reduced [10-16].

Utilization of hollow-section reinforced concrete beams is vital in structural engineering due to its benefits in reduction quantities of concrete used, reduction in overall weight of buildings and superior benefit of passing the electro-mechanical piping system and keep them safe against environmental exposure [17].

The structural behavior of hollow beams has been comprehensively studied by several researchers. The impact of the hollow section's size, form, and location on the flexural response of RC beams has been studied in the past. Literature has employed a variety of concrete kinds as traditional, reactive powder concrete, self - compacted concrete, fiber-reinforced concrete, etc. The findings revealed that creating an opening in the lower area of the beam has little to no influence on its structural capacity, and large openings reduce the capacity compared to the smaller opening [17-21]. The effect of single, double and multiple longitudinal cells has been investigated. The findings revealed that there were an improvement in load carrying capacity for beams with double and four cells compared to single cell [22].

The deterioration of civil infrastructure results from a combination of environmental and operational factors. In bridge structures, exposure to severe seasonal temperature variations, repeated freezing and thawing cycles, and the application of deciding chemicals are among the primary causes of gradual structural degradation. These conditions can accelerate material deterioration and reduce the service life of bridge components. In addition, increasing traffic volumes and heavier vehicle loads impose significant stress on bridge elements. Insufficient maintenance practices and accidental impacts from vehicles or vessels can further aggravate structural damage, resulting in reduced overall performance and durability of bridge systems [23]. Structural rehabilitation of buildings is often necessitated by factors such as changes in occupancy requirements, earthquake-induced damage, blast and impact actions, and the long-term deterioration of construction materials resulting from environmental effects and aging. Corrosion of steel reinforcement is one of the primary durability concerns in reinforced concrete structures that can adversely affect structural integrity and serviceability. To address these challenges, Fiber-Reinforced Polymer (FRP) compounds are widely utilized to strengthen and retrofit structural components. The widespread use of FRP materials is primarily due to their exceptional mechanical performance, characterized by a great strength/weight proportion, lightweight nature, superior resistance to erosion, and straightforward installation procedures. Additionally, FRP strengthening systems generally eliminate the need for formwork, thereby reducing construction time and facilitating efficient rehabilitation of existing structures.

FRP strengthening is primarily implemented through two approaches: the Near-Surface Mounted (NSM) technique, which places FRP bars or strips in grooves within the concrete cover, and the Externally Bonded (EB) technique, which uses adhesive to attach FRP sheets to the concrete surface [12]. The problem in FRP strengthening is the debonding of FRP laminates. Numerous studies have investigated different methods for improving the strength of the link between the concrete bottom and FRP laminates. Danraka et al. 2017 [24] have evaluated different failure modes associated with FRP-strengthened beams and proposed several strengthening and rehabilitation techniques for RC beams using CFRP composites. Finite element simulation has been proposed to predict the experimental results. Rageh et al. 2022 [25] studied bonding of GFRP laminates using either epoxy risen or geopolymer. The comparison revealed the efficiency of geopolymer technique. Moreover, a finite element modelling has been proposed using ABAQUS to predict experimental results. As for hollow beams exhibiting a reduction in bearing capacity, several published studies have examined the impact of FRP strengthening on the structural behavior of hollow beams. Experimental research was done on the bending acting of self-compacting hollow concrete beams having cast-in-place circular holes at various locations.

Several CFRP strengthening schemes were employed to assess their effectiveness in enhancing the beams' load-bearing capacity and structural performance, Hemzah et al [26]. An investigation was conducted keen on the flexural performing of hollow section beams with different opening dimensions. Strengthening was achieved using CFRP sheets bonded to the beam soffits and additional U-shaped CFRP wraps, and their influence on flexural capacity was assessed, Sirisonthi et al. [27]. The bending response of hollow concrete beams was assessed after strengthening the tensile zone with externally bonded reinforcement arranged as either continuous straight laminates or U-shaped wraps. The retrofitting materials included ferrocement and FRP laminates, while CFRP and GFRP composites were selected to associate the efficiency of different composite strengthening systems., Shaheen et al. [28]. Kavitha et al. [29], inspected the bending response of T-beams fortified using GFRP laminates in different configurations, CFRP sheets attached to the soffits of the beams, besides U-shapes bonded to the beam. Alobaidi and Al-Zuhairi [30], examined the efficiency of FRP strengthening utilizing CFRP on the bending and shear responses of reinforced concrete T-beams.

Ravindra et al. [31], compared the bending behavior of CFRP-strengthened T-beams using the EB and NSM strengthening techniques.

Negative bending moments are typically observed in T-beams functioning as inverted sections cast integrally with the slab or in continuous RC beams at support locations, as shown in Figure 1). Studies addressing the behavior of continuous T-beams in negative moment regions are still scarce. Nevertheless, according to the ACI requirements, while designing and analyzing T-beams subjected to negative bending moments (i.e., once the flange is in tension), certain constraints should be taken into account [32].

An analytical investigation utilizing finite element modeling was suggested by Abbas and Ameen [33, 34] to investigate the validation of ACI (24.3.4), with a comparison of an experimental beam specimen. In accordance with the ACI (24.3.4), the results displayed that up to 33% of flexural steel might be dispersed above the flange breadth, but not more than (ln/10).

The strengthening of negative moment regions in reinforced concrete beams presents greater challenges than that of positive moment regions, owing to the concurrent occurrence of large bending and shear stresses at the same regions. Furthermore, the presence of columns in these regions may restrict the implementation of the strengthening system. The flexural response of full-scale RC T-beams strengthened with CFRP laminates at together negative as well as positive moment zones was examined by Al-Khafaji and Salim [35]. Haryanto et al. [36], presented an analytical model to evaluate the value of strengthening reinforced concrete T-beams in negative bending moment areas using half-embedded NSM-CFRP rods. An analytical validation was proposed using a response-2000 is, a program that uses the improved compression field principle to analyze how well the steel wire rope approach affects the bending behavior of RC T- beams. Haryanto et al. [37] used outside welded steel wire ropes to reinforce these beams in the negative moment area. Bank et al. [38], investigated the impact of FRP strengthening on the structural behavior of RAC beams under shear and flexural loading by employing a strengthening scheme consisting of CFRP longitudinal shreds bonded to the enclosed ring wraps and beam soffit. Furthermore, the impact of strengthening on the flexural reaction of RCA beams with different RCA concentrations was assessed by Ftnan and Makki [39].

As for recycled aggregate concrete structural elements, which exhibited low performance, an alternative approach to utilizing RCA in structural members is to restore or enhance their performance through external strengthening. Because of their exceptional strength-to-weight ratio and resistance to corrosion, Fiber Reinforced Polymer (FRP) composites are now widely considered the industry standard for structural retrofitting. While Carbon FRP (CFRP) is widely researched, Glass FRP is for certain applications, Glass Fiber Reinforced Polymer (GFRP) provides an extra economical substitute.

When strengthening RCA concrete with FRP, a recurring issue is premature failure caused by the laminate peeling away from the underlying concrete substrate. The "weak link" is often the concrete surface itself; for RCA concrete, the surface layer may be particularly prone to separation. To mitigate this, the Externally Bonded Reinforcement on Grooves (EBROG) technique has been proposed. By cutting grooves into the concrete cover, the EBROG method increases the bonding surface area and provides mechanical interlock, potentially bypassing the weak surface mortar layer. The EBROG (Externally Bonded Reinforcement on Grooves) and EBRIG (Externally Bonded Reinforcement in Grooves) methods have been developed as substitutes for conventional application techniques [40-44].

1.1. Problem statement and research significance

In conclusion, the previous literature review of the relevant literature, full-scale reinforced concrete beams with large longitudinal opening has not be fully covered in the literature [27], where the longitudinal opening has a significant effect on reducing the weight of RC beams due to the reduction in concrete quantities and thus reducing the cost of the structure. The need for more sustainable alternatives has encouraged utilizing the recycled concrete aggregate for structural applications. The demand for strengthening of RC structures is becoming more important. Hollow beams exhibiting less performance than solid beams, so the need for strengthening is important. Negative moments in beams have not been fully covered in the literature. While CFRP strengthening is well-documented, the efficiency of cost-effective GFRP combined with the EBROG technique specifically for hollow-core RCA beams, which are prone to surface weakness, remains unexplored. This study addresses a specific gap in the literature: the behavior of hollow-core T-beams in the negative moment region. While hollow-core beams are advantageous for reducing dead load and accommodating utility services, and T-beams are ubiquitous in continuous floor systems, the negative moment behavior (where the flange is in tension) of such complex sections containing RCA remains under-researched. Existing studies largely focus on positive moment regions or solid sections. Therefore, this research aims to evaluate the flexural efficiency of full-scale hollow-core RCA T-beams strengthened by GFRP using the EBROG technique. The study examines the interplay between RCA replacement ratios (0%, 50%, and 100%) and the efficiency of the strengthening system, providing novel experimental data on the viability of sustainable, lightweight, and strengthened concrete members in critical support regions.

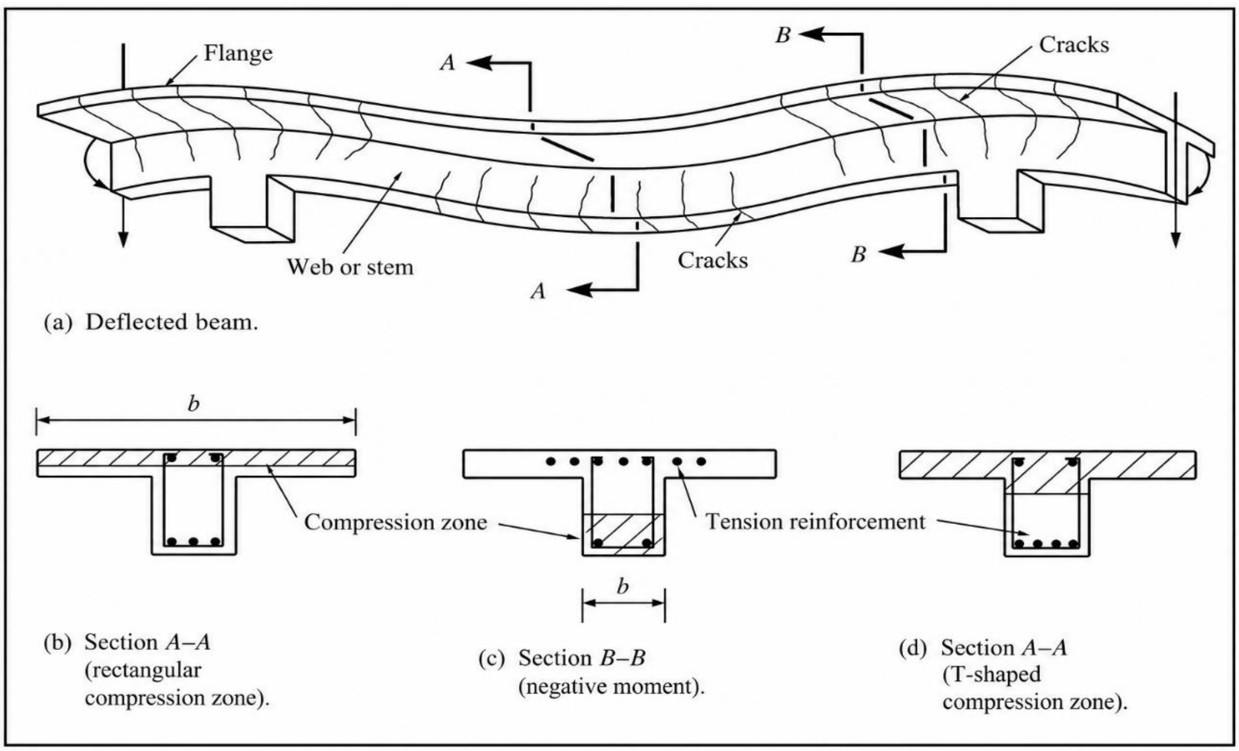

Fig. 1 Positive and negative moment regions in a T-beam[45]

2. Work of Experimental

2.1. Materials

2.1.1. Coarse Aggregate

Natural Coarse Aggregate

A naturally rounded, well-graded gravel utilizing a maximum size of 14 mm that complies with BS 882 (1992) [45].

Recycled Concrete Aggregate

The recycled aggregate has been prepared from the demolition-tested cubes collected from the testing lab in the college campus, Figure 4. Waste cubes were of good-quality concrete. They were crushed utilizing a chops crusher, after which the aggregate was cleaned, dried, and classified to a maximum size of 14 mm in accordance with [45].

Physical properties and grading requirements are presented in Table 1 and Figure 4.

Fig. 2 Waste testing specimens

2.1.2. Fine Aggregate (sand)

Washed river sand is used as fine aggregate. The grading requirements conformed to British Standard BS 882-1992 [46]. Physical properties and grading requirements are presented in Figure 3.

2.1.3. Cement

Ordinary Portland cement (OPC), wherever its properties meet the IQS No. 5/1984 [47].

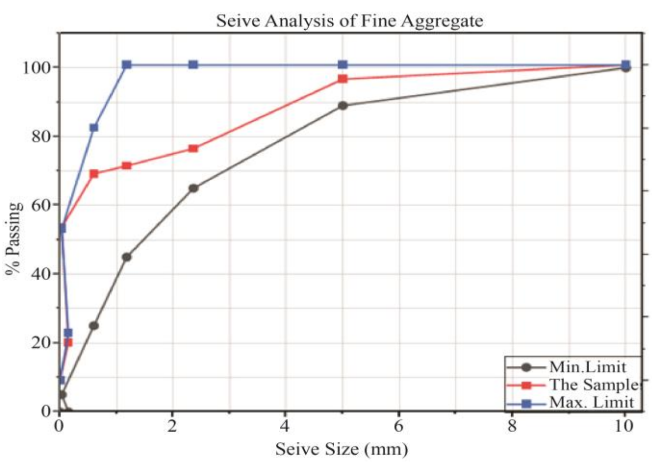

Fig. 3 Sieve analysis of coarse aggregates

2.1.4. Water

Clean water, free of organic materials, turbidity, and dissolved salts, was utilized in the preparation and curing of concrete specimens and maintained at a temperature of 20 ± 2°C.

2.1.5. Reinforcing Steel

Deformed steel bars were used in diameters of (6, 8 and 10) mm. Three samples of each bar size were tested in the laboratory according to ASTM A 615 [48]. The test results are revealed in Table 2.

2.1.6. Strengthening Materials

GFRP grids with epoxy resin have been used as an externally bond strengthening. The properties of epoxy and GFRP sheet are presented in Table 3, obtained from the manufacturer's data sheets.

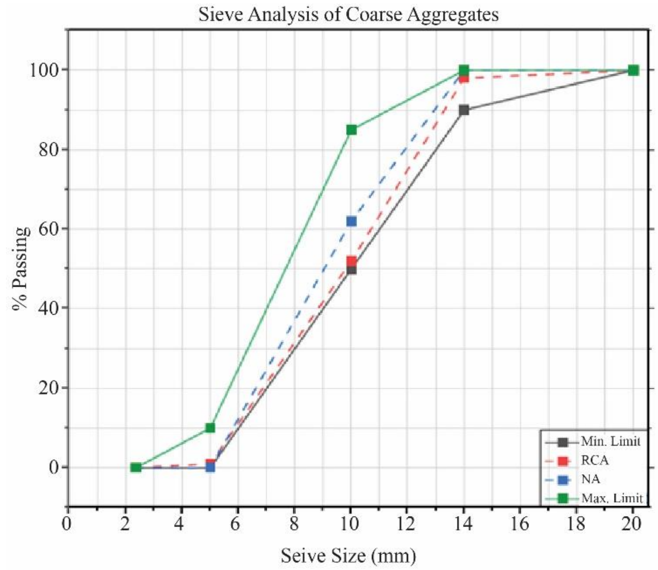

Fig. 4 Sieve analysis of fine aggregate

2.2. Concrete Mixes

A control concrete mix has been designed according to simplified mix design – the British DOE method (1988)[49, 50], to get an objective compressive strength of (35 MPa). For other mixes, coarse aggregate is replaced by (50 %) and (100 %) RCA by weight of total aggregate. The presence of free water substantially influences the properties of concrete in together its hardened and fresh conditions. Because Recycled Concrete Aggregate (RCA) exhibits higher water absorption due to residual mortar on its surface, both the Natural Aggregate (NA) and RCA were washed and submerged in water for 24 hours. The excess water was then drained to achieve a Saturated Surface Dry (SSD) state as stated by the DOE method. Mixing water has adjusted in the laboratory according to the saturation level of the aggregate. The absorbed water was not included in the calculation of W/C content to ensure sufficient water needed to complete the hydration of cement in concrete mixes. The compressive strength measured based on cubic specimens (150 * 150 *150) mm. Cylinder compressive strength is approximately 80 % of cube compressive strength for the same mixture [50]. Properties of all mixes are presented in Table 4 and Figures (5), (6) and (7).

2.3. Full-Scale Beam Specimens

A total of six hollow core T-beams has been manufactured and tested to evaluate the main variables of this study. The beams were fabricated using various contents of RCA as a replacement of the total coarse aggregate weight. The beams' overall length is 3600 mm, and their effective span length is 3200 mm. All beams' cross-sections consist of total depth of (300 mm), (400 mm flange width), (100 mm flange thickness) and (200 mm web width). Beams have been divided into 2 groups, the first group (Group One) contains of three beams utilizing three substitute proportions of RCA, 0 %, 50

% and 100 %, and they were denoted by (U-INVE-HTB-X), where U represents (Unstrengthened), INVE represent the situation of testing (inverted), HTB represents (Hollow T-Beam) and X represents the replacement ratio. The second group same as the first group, but with GFRP strengthening on the top surface of the flange, and they were denoted by (ST-INVE-HTB-X), ST means strengthened beam. The beams have been designed in accordance with ACI 318. The main reinforcement of RC beams consisted of eight bars with a diameter of (9.5 mm) with a nominal yield strength of (754 MPa). To prevent shear failure, six millimeters diameter stirrups at a spacing of (100 mm) were used, having a yielding strength of (486.26 MPa). Two 8 mm steel bars were added at the top to keep the stirrups vertically aligned. A strain gauge was affixed to 2 steel bars at the center of every RC beam. Concrete spacers placed under the reinforcing cages to maintain a 30 mm concrete cover. To create the longitudinal cavity, a polystyrene foam strip with a section dimension of 120 mm × 75 mm was secured using small steel bar pieces to maintain its position and prevent it from floating during concrete casting and vibration. All beam details are presented in Figure (7).

Table 1. Properties of coarse aggregates

Aggregate Type	Bulk specific gravity (SSD)	Bulk Density (Kg /m^3)	Absorption (%)	Density (Kg/ m^3)
NA	2.66	1700	1.0	2660
RCA	2.42	1310	4.56	2420

Table 2. Properties of steel reinforcement

No.	Ultimate strength (MPa)	Yielding strength (MPa)	Modulus of elasticity (GPa)	Elongation (%)
Ø6 mm	589.16	486.26	200	5.183
Ø8 mm	541.746	436.533	200	7.80
Ø 10 mm	858.54	754.163	200	9.617

Table 3. Properties of GFRP and Epoxy

GFRP	**Tensile Strength (MPa)**		**Modulus of elasticity (MPa)**	
	715		2800	
Epoxy	Tensile Strength (MPa)	Modulus of Elasticity in Flexure (MPa)	Modulus of Elasticity in Tension (MPa)	Tensile Strain at Break
	30	3800	4500	0.9 %

Table 4. Concrete mixes properties

Mixture	Design Strength (MPa)	Slump (mm)	W/C	Measured Strength (MPa)		% change in f'_c
				cube	cylinder	
0 % RCA	35	70	0.39	42.5	34	-----
50 % RCA	35	47	0.39	43.11	34.50	+1.5 %
100 % RCA	35	45	0.39	49.2	39.36	+ 16 %

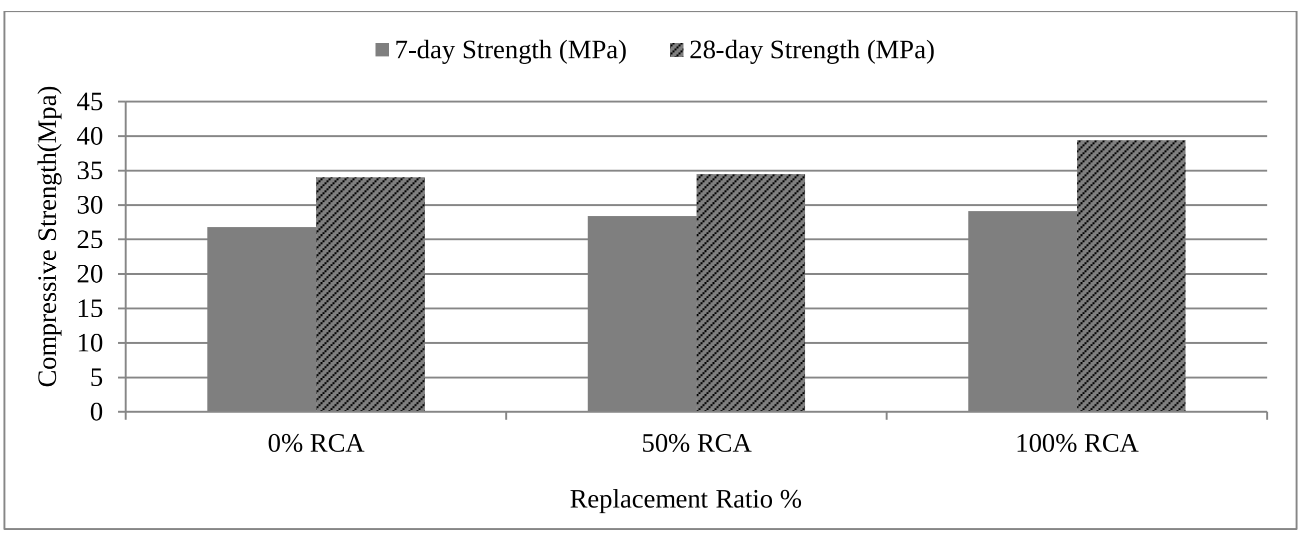

Fig. 5 Compressive strength versus percentage of RCA

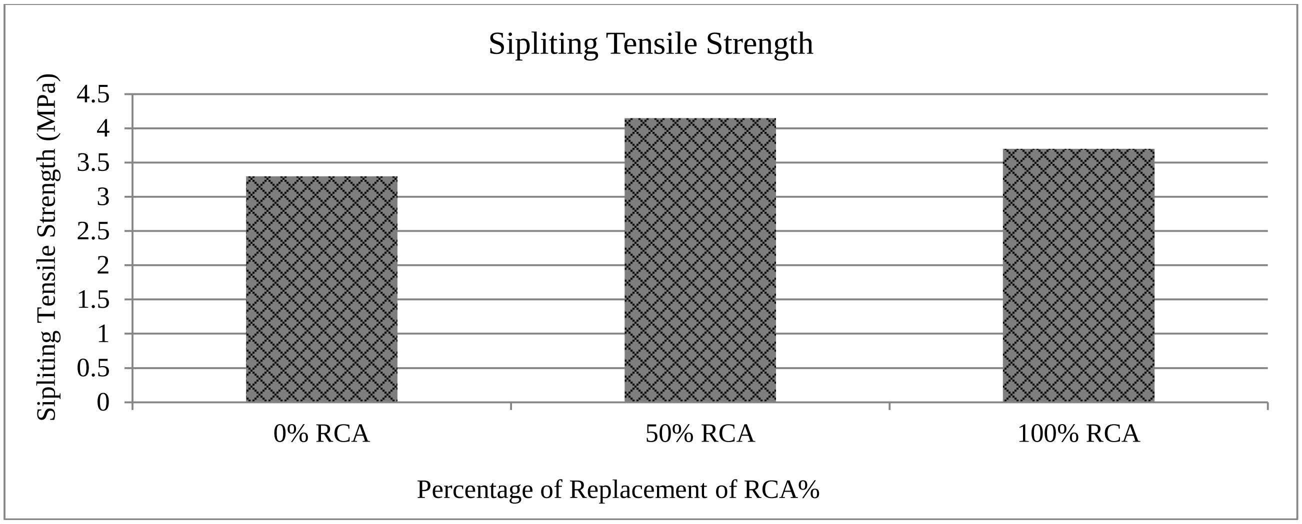

Fig. 6 Splitting tensile strength of concrete versus percentage of RCA replacement

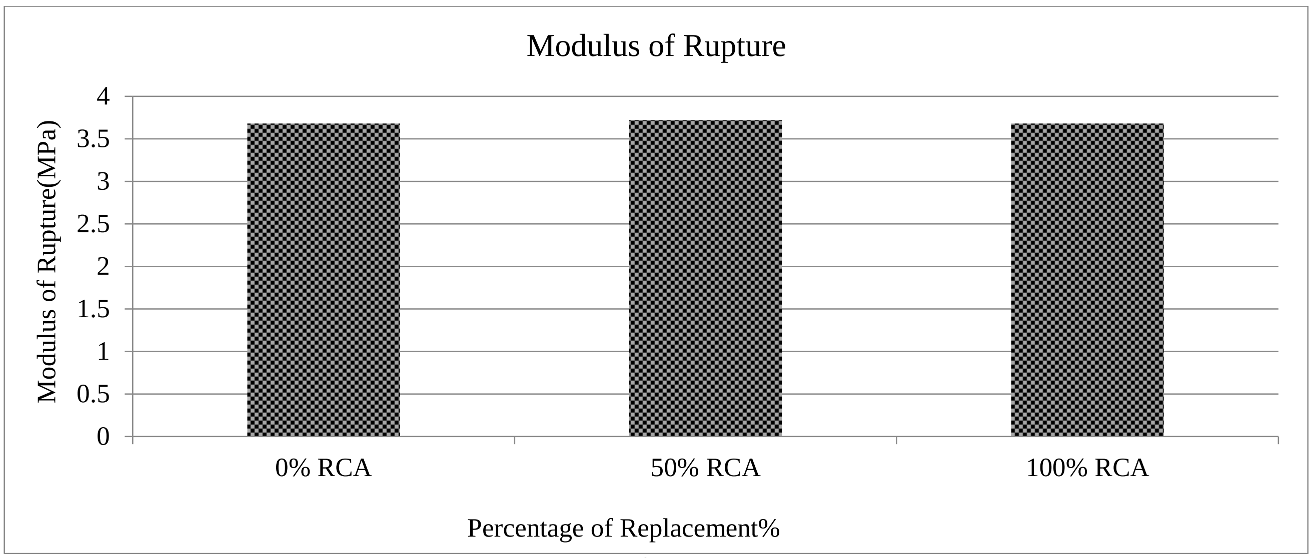

Fig. 7 Modulus of rupture test results

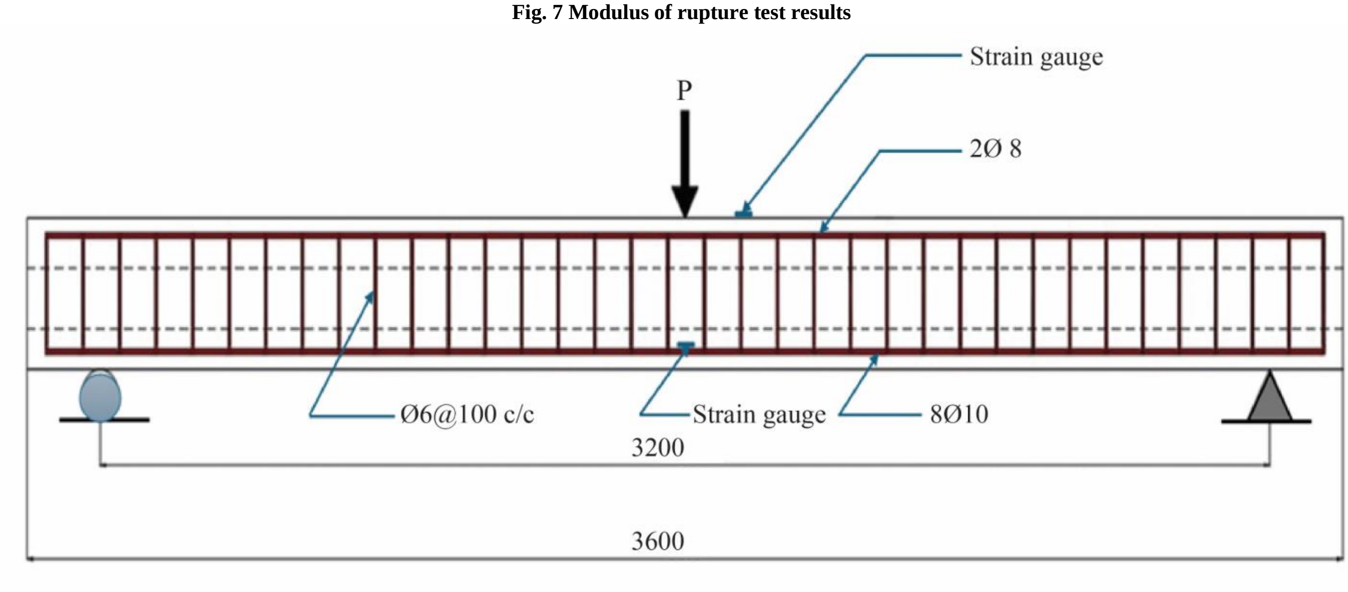

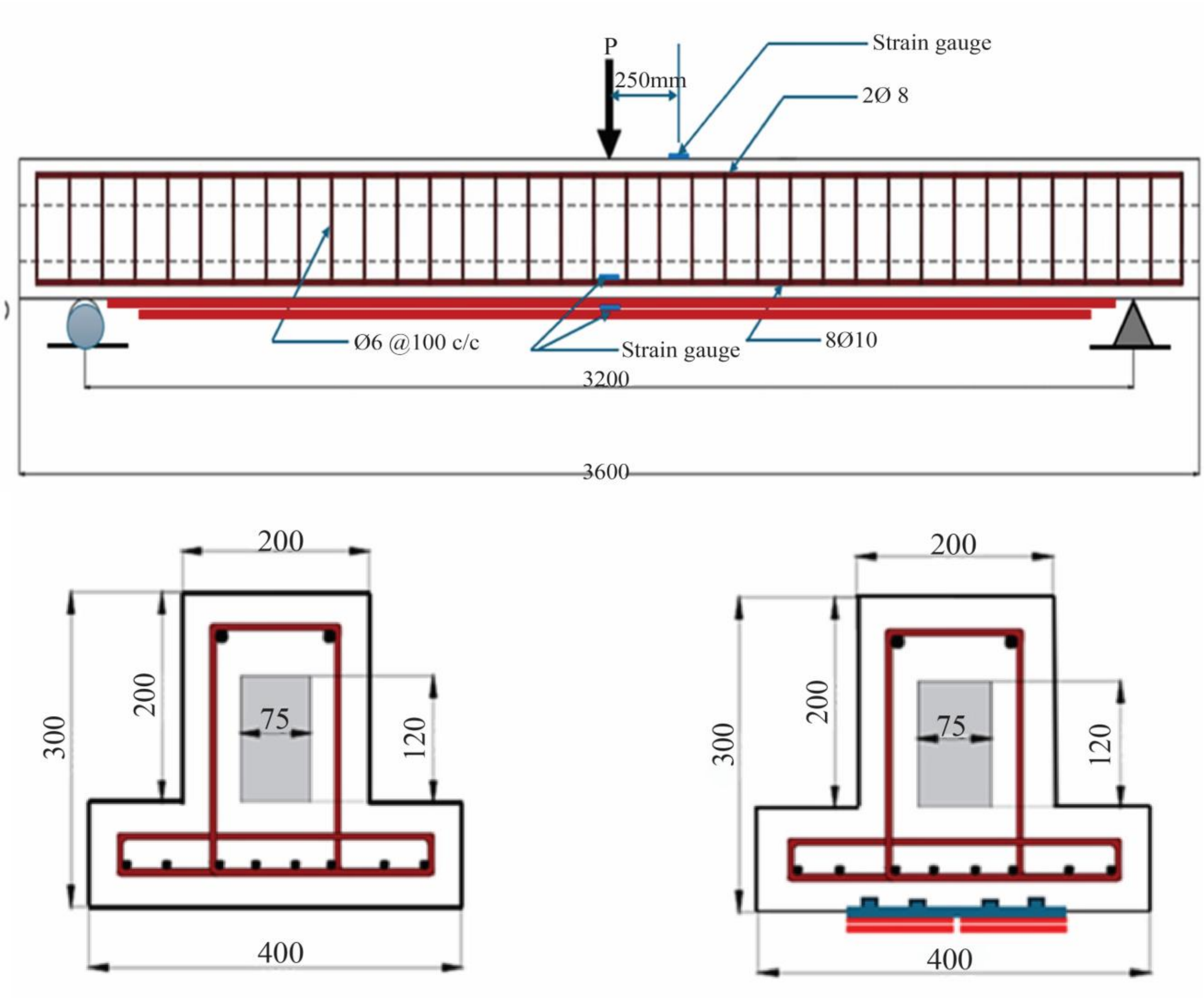

Fig. 8 Details of RC T- Beams

2.4. Procedure of bonding GFRP

GFRP bonding process was established following the guideline presented by the (ACI 440.2R-23) [51]. Top surfaces of the flanges were cleaned and prepared. Four longitudinal grooves were located using a marker to a length of (3100 mm), then an electric cut device by means of steel blades was utilized to form longitudinal channels in the concrete cover with dimensions of (10 mm* 10 mm). Prior to installing the GFRP grids, the concrete substrate was ground, water-blasted, and dried to ensure a clean and moisture-free surface. The GFRP sheets were then cleaned and cut into tapered strips, each 100 mm wide and of different lengths, following the recommendations of ACI 440.2R-23 (Section 12.1.2) [51]. The initial layer's length (3100 mm) matched the groove's length, whereas to provide a 150 mm gap on each side, the second layer's length was (2800 mm). After the surface preparation, the epoxy resin and hardener were made by combining them in a ratio of one part hardener to four parts resin.

Then, a prime coat of epoxy applied prior to filling the groove, epoxy was put in place to guarantee that the epoxy has completely penetrated the concrete surface. The wet layup technique was employed, in which epoxy was used to entirely fill the grooves before the GFRP strips were immediately installed.

The strips were applied progressively from one end to the other along the groove length while applying slight pressure to ensure that the epoxy filled the spaces amongst the GFRP shreds and the groove sides and to eliminate any entrapped air. After strengthening, before testing, beams were given seven days for curing.

A strain gauge was installed between the GFRP layers at each beam's central to determine the performance of the FRP strengthening during the test. Steps of casting, preparing and strengthening of beams are revealed in Figure (8).

Fig. 9 Preparing of RC T-beams

2.5. Beams Set-Up and Instrumentation

The beams painted white color to show the deformations and cracks while testing. All beams were simply supported and were tested as an inverted beam were the flange in tension simulate the negative moment region of continuous beams. Three-point bending tests were performed where the central point load represents the column support. The upper surface of the beam at mid-span experiences the greatest compressive strain in the concrete, a strain gauge was positioned 250 mm away from the mid-span to avoid potential damage subsequent from the load application device. The load was put on directly at the central at rate of 2-4 kN/min. To measure the beam's deflection, 2- LVDTs were positioned at the mid-span. The beam set-up is presented in Figure (10).

3. Experiment Results and Discussion

3.1. The Non-Strengthened Beams

3.1.1. Load-Deflection Responses

The load-deflection responses for the non-strengthened specimens (Group One), as revealed in Figure 9. All beams exhibited a typical trilinear behaviour: uncracked elastic stage, cracked elastic stage, and post-yield plastic stage. Interestingly, the final load-carrying capacity was little impacted negatively by the addition of RCA. The ultimate load attained by the 100% RCA beam was similar to that of the natural aggregate control beam. However, the post-cracking stiffness was affected; beams with RCA exhibited larger deflections at equivalent loads associated to the reference beam.

According to the experimental outcomes, utilizing recycled concrete aggregate increased beam deflection and slightly reduced yield load compared to the natural aggregate beam, as observed from the yield and ultimate load measurements shown in Table 5. Compared with the natural aggregate concrete beam, the beam incorporating 50% recycled concrete aggregate showed a 1.9% reduction in load-carrying capacity, while the beam with 100% RCA demonstrated a similar capacity. However, the corresponding deflections increased by about 34% and 38% for the 50% and 100% RCA beams, respectively. This increase in deflection is consistent with the lower elasticity modulus typically associated with RCA concrete, as the porous residual mortar increases the deformability of the aggregate skeleton.

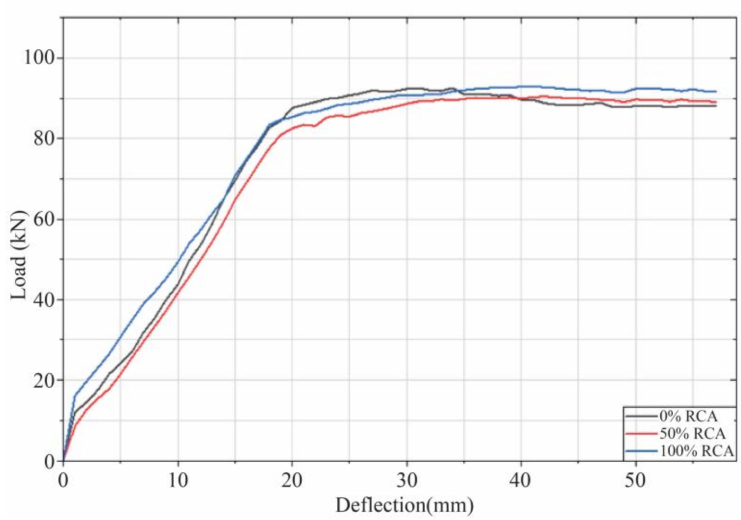

Fig. 10 The deflection vs load of the unstrengthen beams (Group One)

Table 5. Experiment results of non-strengthened beams

Beam Name	P_{cr} (kN)	P_{yield} (kN)	P_{max} (kN)	Deflection (mm)			% rise of P_{max}
				Δ_{cr}	Δy	Δu	
U-INVE-HTB-0	14	88.94	93.39	1.9	21.42	32.17	-----
U-INVE-HTB-50	11	82.77	91.59	2.49	22.40	43.09	-1.9
U-INVE-HTB-100	14	84.57	93.40	2.98	21.42	44.32	+0.0

3.1.2. Failure Modes and Crack Pattern

Figures (11-13) illustrate the failure modes of the tested beams. All specimens unsuccessful the flexure test, with the dominant cracks developing beneath and adjacent to the concentrated load at the central section. These cracks originated from the bottom surface of the inverted flange and propagated upward toward the top of the beam, widening progressively as the applied load increased until failure occurred. All beams exhibited a ductile manner of failure, characterized by yielding tensile reinforcement prior to severe of the concrete in the compression zone; therefore, no compression failure was observed. Furthermore, diagonal cracks appeared when the applied load reached approximately 80–95% of the maximum load.

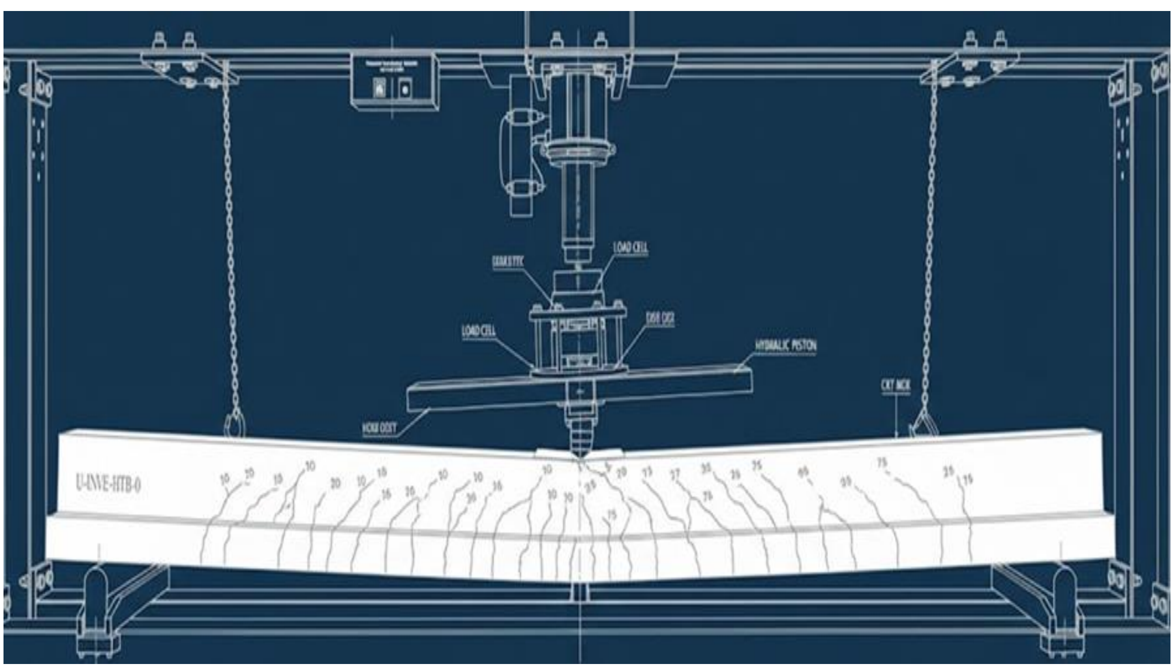

Fig. 11 The beam set-up

Fig. 12 Beam failure mode (U- INVE-HTB-0)

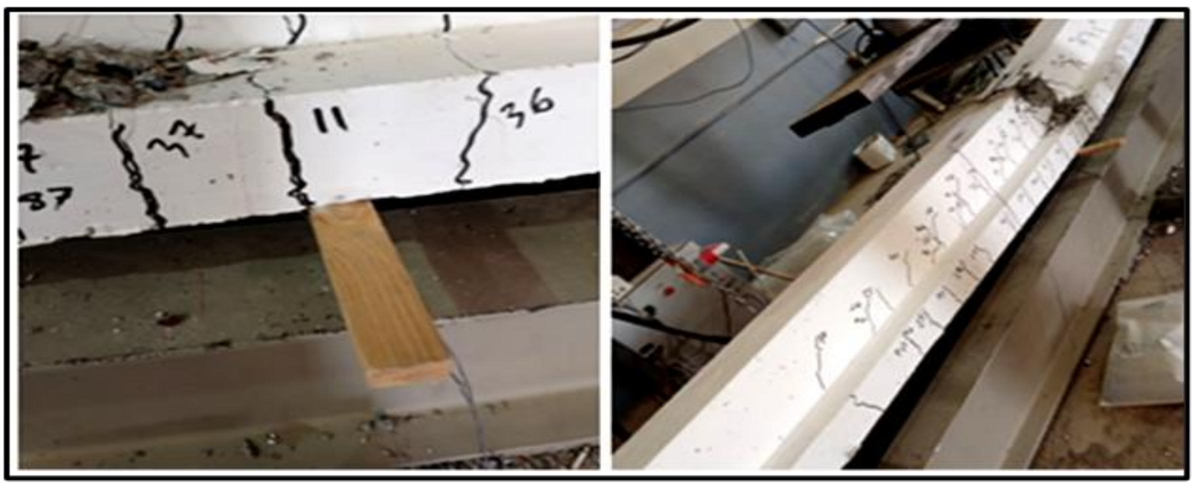

Fig. 13 Beam failure mode (U- INVE-HTB - 50)

Fig. 14 Beam failure method (U- INVE-HTB - 100)

3.2. GFRP Strengthened Beams

3.2.1. Load vs Deflection curves

The beams' test (strengthened) results are displayed in Table (6) and Figure (14). Figure (14) illustrates the load vs deflection curves for all specimens, reflecting their flexural behavior from the onset of loading to ultimate failure. In the elastic range, all beams showed similar responses. Furthermore, the strengthened beams exhibited nearly equivalent load-carrying amounts, as indicated in Table (6). Regarding to deflection, the beam incorporating 50% RCA recorded a decrease of approximately 12.3%, while the beam with 100% RCA experimented an increase of about 14% relative to a beam cast with normal coarse aggregate. This trend is evident from the deflection values recorded in Table (6).

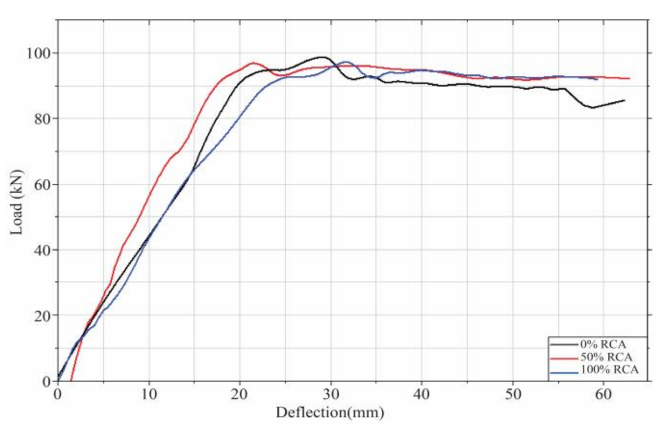

Fig. 14 The load-deflection of RC beams (Group Two)

Table 6. Test outcomes of strengthened experimented beams

Beam Name	P_{cr} (kN)	P_{yield} (kN)	P_{max} (kN)	Deflection (mm)			% reduction of P_{max}
				Δ_{cr}	Δ_y	Δ_u	
ST-INVE-HTB-0	10	86.84	99.34	1.99	18.92	28.39	--
ST-INVE-HTB-50	10	87.51	98.05	1.94	17.93	24.90	-1.3
ST-INVE-HTB-100	11	86.57	98.55	1.99	18.09	32.38	-0.8

3.2.2. Crack Patterns and Failure Modes

Figures (15-17) demonstrate the reinforced beams' failure modes and crack dispersion. All specimens failed in flexure, with pronounced flexural cracking developing beneath and near the concentrated load. These cracks extended upward toward the compression zone and became more extensive with increasing load. Furthermore, diagonal cracks appeared at load levels ranging from approximately 80% to 95% of the ultimate load. The governing failure way was rupture of the GFRP strengthening system, go together with yielding steel reinforcement. In about locations, particularly in the beam with 50% RCA replacement, partial delamination of the GFRP was detected. The failure manners of all beams was ductile, as the reinforcing steel yielded before concrete crushing occurred in the compression region.

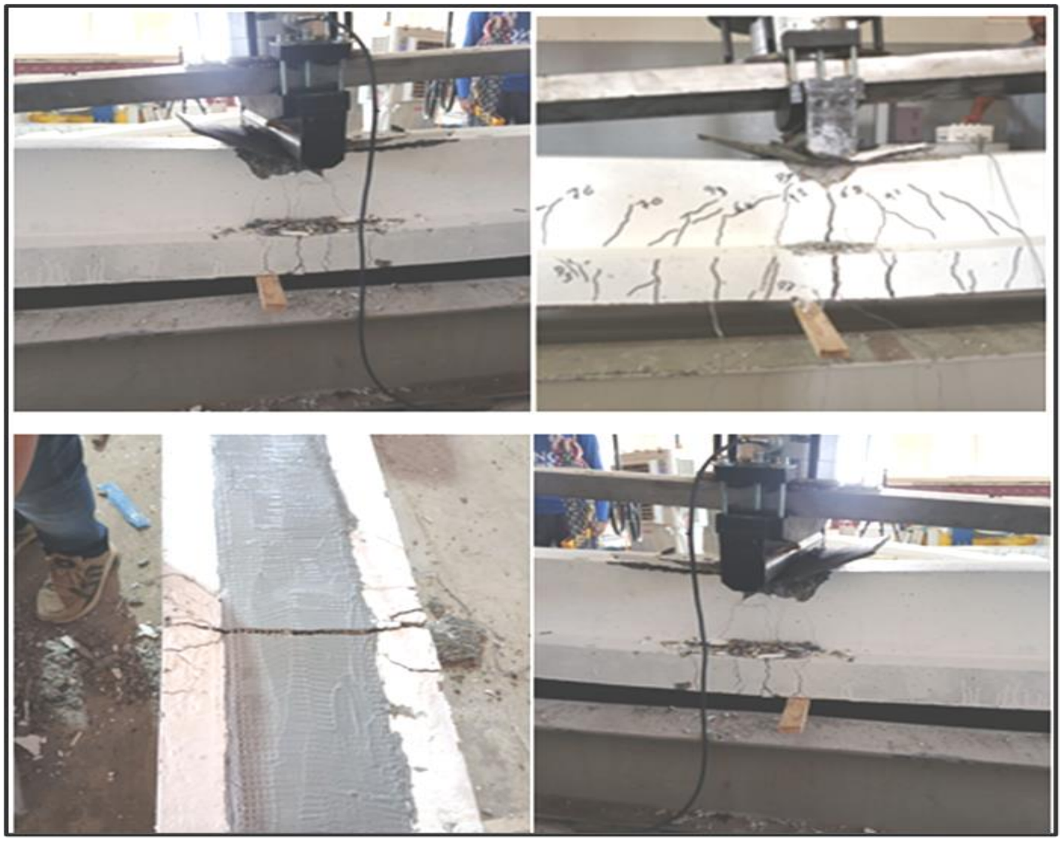

Fig. 15 Failure method of beam (ST- INVE-HTB-0)

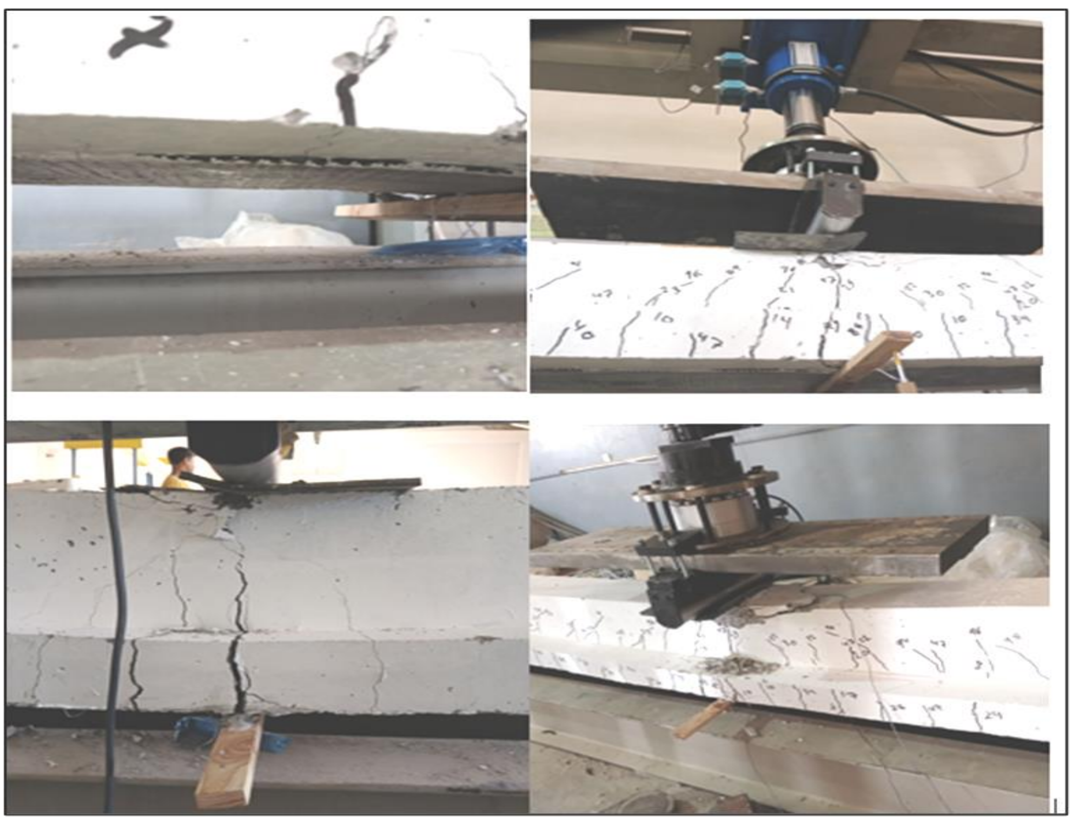

Fig. 16 Beam failure mode (ST- INVE-HTB-50)

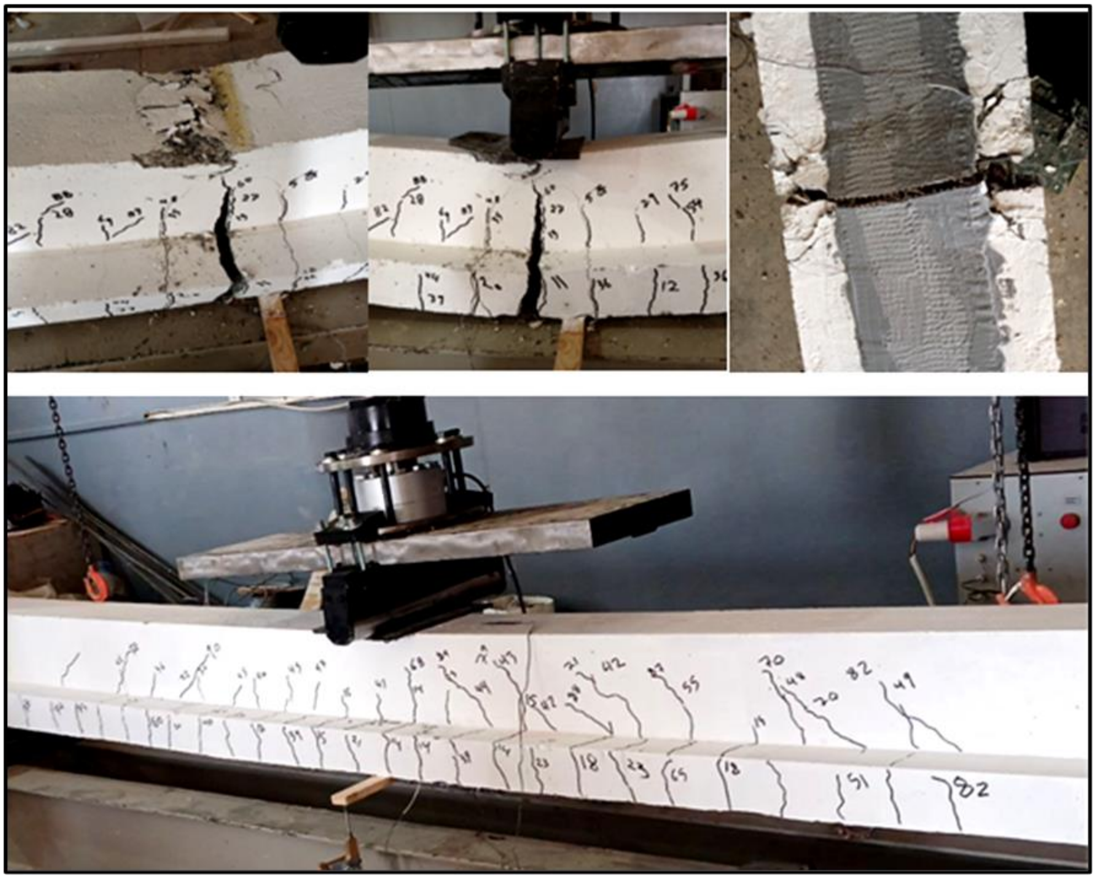

Fig. 17 Beam failure mode (ST-INVE-HTB-100)

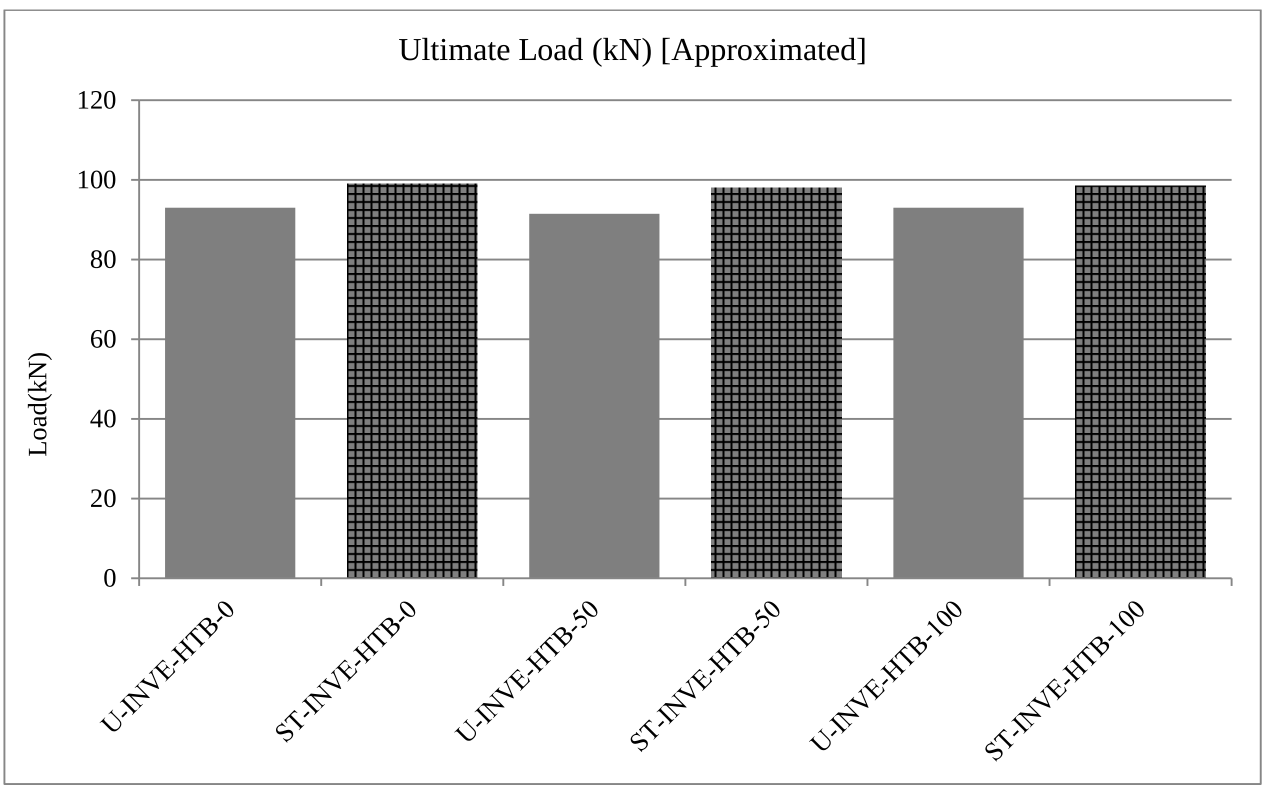

Fig. 18 The load carrying value of all experimented beams

3.3. Effect of FRP Strengthening on RC T-Beams

The application of GFRP sheets via the EBROG technique resulted in a consistent enhancement in flexural performance. As shown in Figure 18, the strengthened beams exhibited an increase in ultimate load capacity ranging from 5.5% to 7.1% compared to their unstrengthen counterparts.

While the percentage increase appears modest, the primary contribution of the EBROG technique was evident in the failure mode. Conventional EBR (Externally Bonded Reinforcement) on RCA concrete often fails via premature debonding of the concrete cover due to the weak surface mortar. In this study, the dominant failure mode for strengthened beams was GFRP rupture rather than immediate debonding. This indicates that the grooves successfully anchored the GFRP grid into the core concrete, bridging the weak surface layer and allowing the composite material to utilize a higher percentage of its tensile capacity before failure. The presence of shear cracks near the supports in beams (strengthened) further confirms that the flexural capacity was enhanced sufficiently to shift stresses toward the shear critical region.

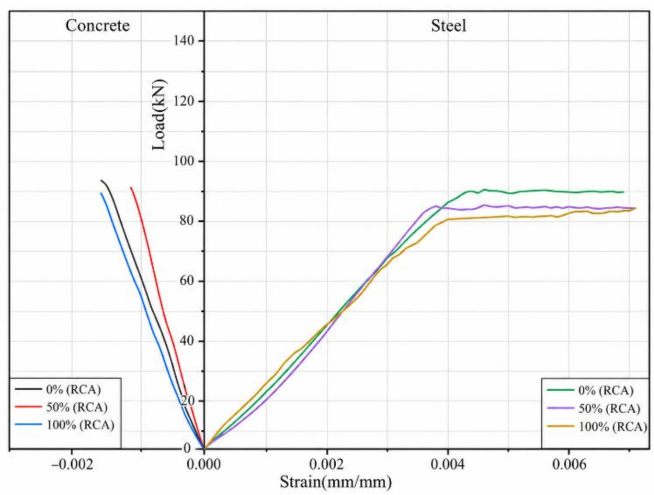

Fig. 19 Load-strain curves of all experimented beams (Group One)

3.4. Load-Strain Relationships

The load–strain relationships of the non-strengthened beams (Group One) were evaluated to examine the effect of Recycled Coarse Aggregate (RCA) on the strain behavior of the concrete and reinforcing steel. The ultimate concrete strain measured in the reinforced concrete beam containing 50% RCA was approximately 33.33% lower than that of the corresponding beam made with natural aggregate. In contrast, the beam incorporating 100% RCA exhibited an increase of approximately 6.67% in ultimate concrete strain. These variations can be attributed to the influence of RCA on the mechanical behavior and deformation characteristics of concrete. For all specimens, the measured concrete strains remained below the ultimate concrete strain limit of 0.003, indicating that concrete crushing did not occur before the maximum load was reached. Furthermore, the load–strain relationships exhibited an approximately linear trend up to the point of strain-gauge failure, as shown in Figure 19.

With respect to the reinforcing steel, the relationship between the applied load and the measured steel strain was consistent with the results presented in Tables 5 and 6 and with the load–deflection curves discussed previously. This consistency indicates that the strain measurements of the reinforcing steel agreed with the overall load-carrying and deformation behavior of the tested beams.

3.4.1. FRP- Strengthened beams (Group Two)

Figure (20) demonstrations the load-strain curves for the strengthened beams (Group Two). Compared with the natural aggregate reinforced concrete beam, the ultimate concrete strain increased by approximately 63.6% for the beam containing 50% RCA and by 18.2% for the beam containing 100% RCA. This behavior reflects the pronounced impact of RCA on the strain response of the beams (strengthened). Additionally, every strain figure that was recorded was less than the final concrete strain of 0.003, that means all beams exhibited ductile failures.

For steel reinforcement, the strain gauge measurements revealed that the load strain relationships coincided with the outcomes revealed in Table 5 and Table 6 and the load-deflection curves revealed earlier.

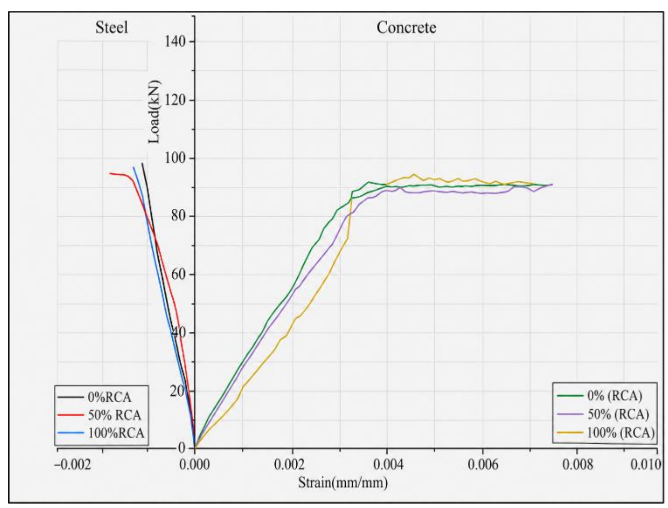

Fig. 20 Load -Strain curve of RC beams (Group Two)

3.4.3. Load-Strain Relationships for GFRP Strengthening

To investigate the performance of FRP laminates during testing, a single concrete strain gauge was placed amongst the two layers of GFRP pieces at mid-span. The strain gauge readings are presented in Figure 21.

Because natural aggregate RC beams have a higher load capacity for carrying than RCA beams, strain gauge is unsuccessful in greater loading as indicated by Lawrence C.

Bank et. al [38]. In this work, strain measurements on the GFRP grids presented in Figure 21 reveal the complex stress distribution within the composite mesh. It was observed that the recorded strains were lower than the theoretical break strain of the GFRP material. This phenomenon is attributed to the geometric nature of the open-grid GFRP mesh used. Unlike continuous fiber sheets, the grid consists of orthogonal yarns. During loading, stress redistribution occurs between individual yarns; rupture often initiates sequentially rather than simultaneously across the width.

Consequently, a strain gauge attached to a single yarn may record values that do not capture the peak strain occurring in adjacent, failing yarns.

Therefore, the strain levels that have been provided should be understood as localized measurements rather than an average strain across the full composite width. This suggests that the actual utilization of the GFRP material may be higher than recorded, confirming the effectiveness of the bond.

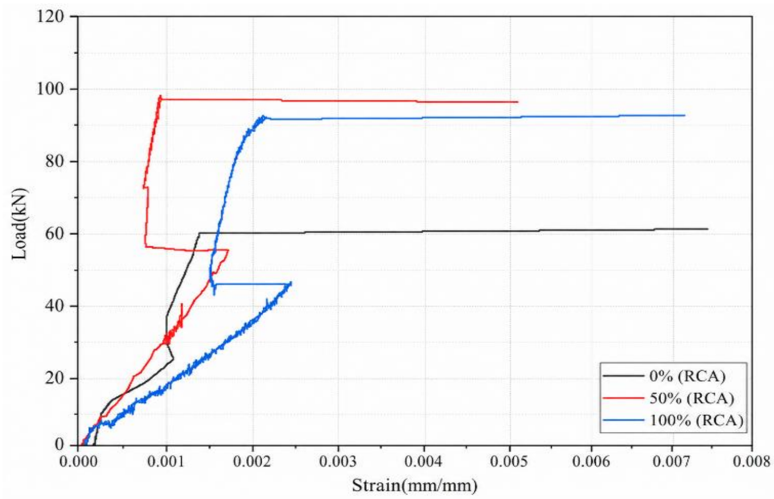

Fig. 21 Load -Strain curves for the GFRP in the strengthened beams

3.5. RC Beams Ductility

Ductility refers to the capability of a material, structural component, or structural system to withstand significant deformations and absorb energy. It is commonly expressed as the ability to undergo substantial plastic deformation while maintaining structural integrity, prior to the occurrence of excessive deformation or failure in one or more structural elements [52]. Ductility could be calculated using the formula accommodating deformations. In other words, the potential of a structure to experience plastic distortion without failing until extreme plastic distortions of a number of parts happen [52]. Ductility could be calculated using the formula

$$\Delta\mu = \Delta u / \Delta y$$

Where;

$\Delta\mu$: the ductility index.

Δu: the maximum deflection.

Δy: the yielding deflection.

The values of ductility

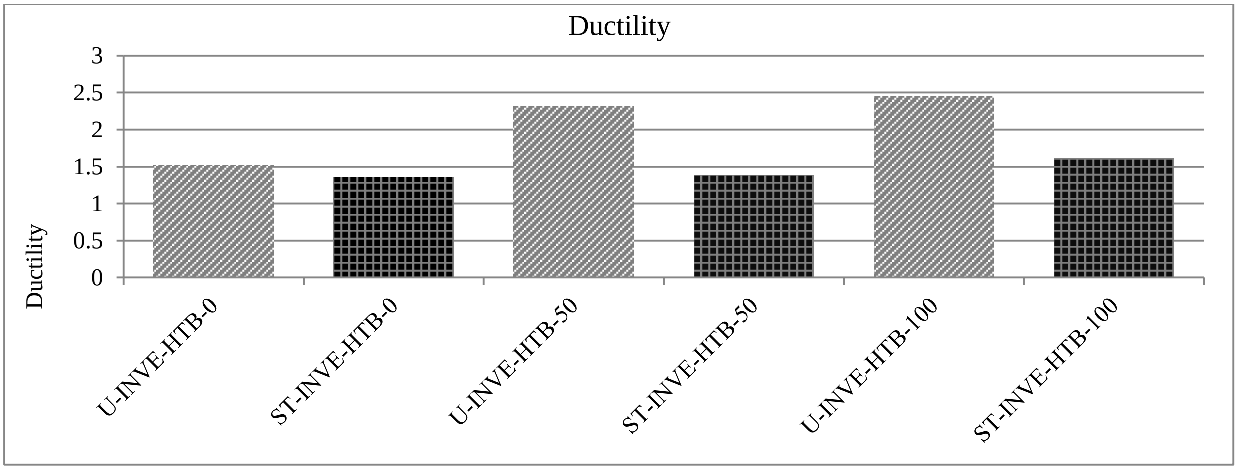

Fig. 22 Ductility of the experimented beams

3.6. Stiffness of Reinforced Concrete T- Beams

Flexural stiffness is obtained through multiplying the moment of inertia by the modulus of elasticity. The load vs deflection graphs of the examined RC beams be able to calculate stiffness experimentally. Various formulas for assessing flexural stiffness have been proposed by authors. As for [54], claimed that RC beam stiffness may be determined by dividing 45% of the maximum load by the equivalent deflection, in accordance with ASTM C 1018-97 . While [2], claimed that the accompanying deflection (Δ_{cr}) divided by the cracking load (P_{cr}) may be used to calculate the stiffness of RC-beams. [53] agreeing to ACI -318 19, the stiffness of RC beam is defined as the inclination of the line between the starting point of the load vs deflection curve to a point that represents a deflection of the beam span's length (L_n/250), which is the great permissible deflection. Herein, stiffness were considered agreeing. Figure 23 displays the stiffness values for each beam. According to the ACI formula, stiffness rises as RCA content increases because concrete's modulus of elasticity rises as RCA content does, increasing concrete's compressive strength.

$$E\_c=4700\sqrt{f_c^{`}}$$

Because the strengthened beams have a greater moment of inertia, the stiffness values for the beams with GFRP strengthening are higher.

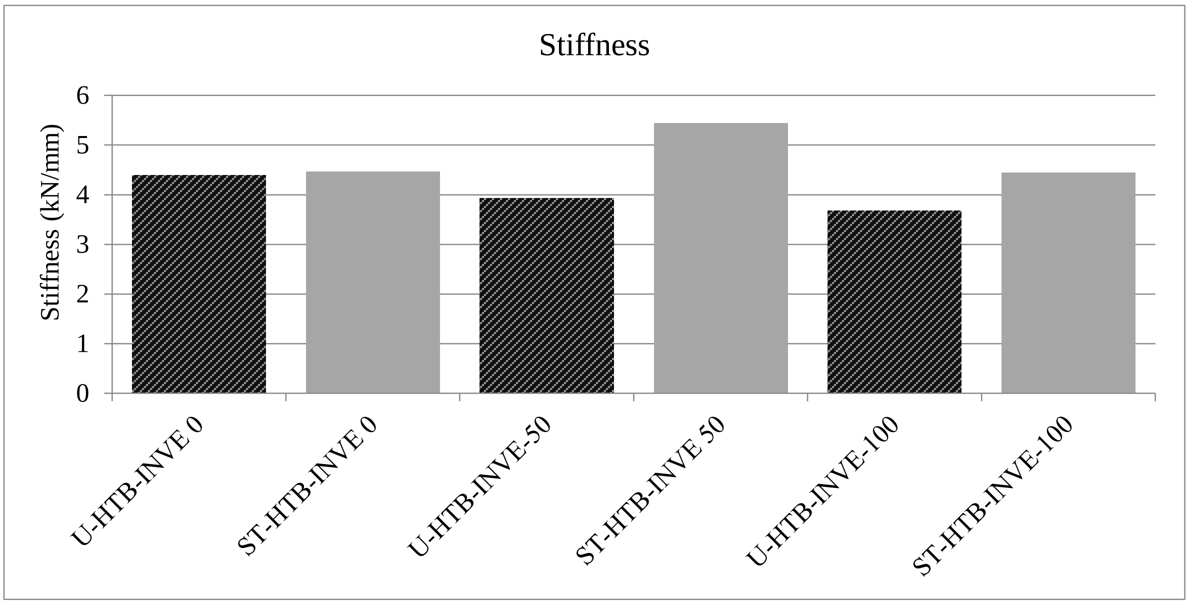

Fig. 23 Stiffness of the tested beams

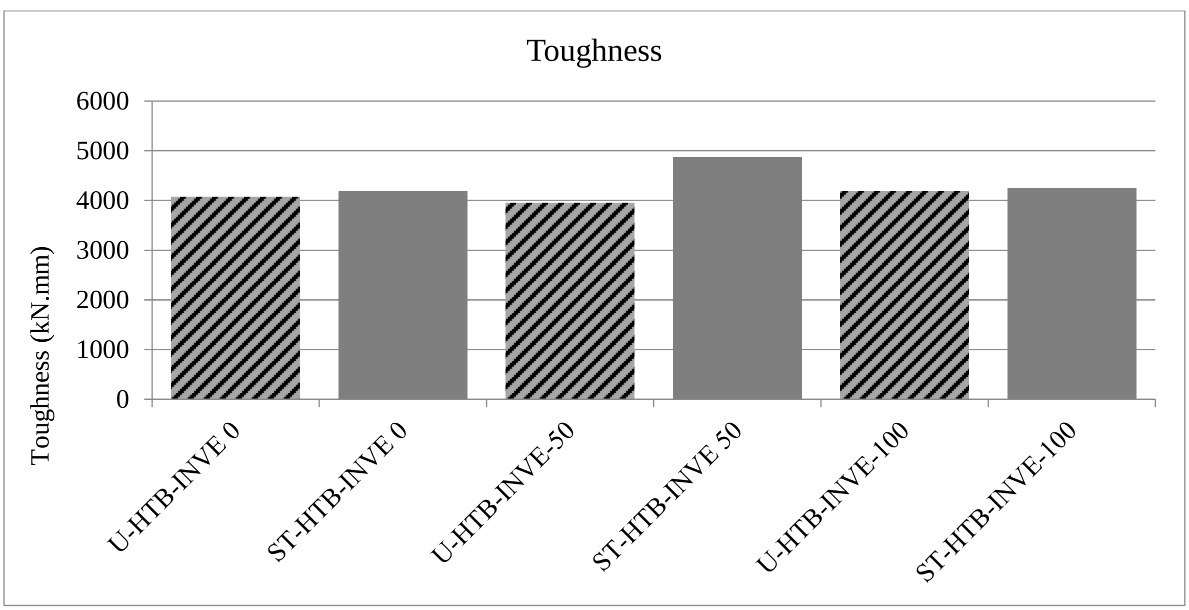

Fig. 24 Toughness of the experimented RC beams

3.7. Toughness of RC T-Beams

Toughness is a material's capacity to absorb energy before fracture and may be expressed as the energy dissipated per unit volume during failure [54]. Alternatively, it can be definite as the total quantity of energy necessary to fracture a specimen [. The toughness of structural members is commonly estimated by computing the region enclosed beneath the load–deflection arc. Since high-strength materials can resist larger loads, they generally produce a greater area under the load–deflection response and consequently possess higher toughness. In this study, toughness values were obtained using the trapezoidal rule and are summarized in Figure 24. The outcomes demonstrate that the strengthened RC beams achieved greater toughness values than the non-strengthened specimens. Toughness values for all beams are revealed in Figure 24.

4. Conclusions

An investigation of the bending performance of RC hollow T-beams using several substitute proportions of RCA has been performed. Three specimens served as un-strengthened beams with different RCA content, while the other three beams were strengthened using. double layers with two strips, 100 mm each. An externally bond FRP strengthening applied using (EBROG) technique. Every specimen underwent a three-points loading test. The experimental results were then verified, leading to the following key findings:

1. There was an enhancement in concrete compressive strength with the rise of RCA ratio in the mixtures up to 16 % for 100 % replacement, as stated in Table 4. This enhancement can be accredited to two main features specific to the materials herein. Initially, tested laboratory cubes gathered from the university site were the source of the RCA. The initial compressive strength of these close relative concrete samples was probably high, possibly more than that of the normal aggregate employed in the control mixture. Second, the rough surface texture of the crushed RCA particles may have improved the mechanical interlock within the new cement matrix. While the high-water absorption of RCA typically poses a workability challenge, it is hypothesized that the internal curing effect or a localized reduction in the operative W/C ratio at the ITZ contributed toward the improved matrix density in the hardened state. Splitting tensile strength of concrete showed a peak at 50% RCA replacement ratio due to unclear behavior of RCA.

As RCA has higher absorption than NA, the absorbed water will participate in hydration, resulting in higher compressive strength.

2. Bending strengthening of reinforced concrete T-beams utilizing GFRP leaves proved to be effective, as the strengthened beam exhibited higher load capacities. Flexural failure mode exhibited for both strengthened and non- strengthened beams, highlighting the effectiveness of GFRP in enhancing structural performance.
3. Stiffness is higher for strengthened RC beams as opposed to non-strengthened RC beams because the strengthened beams' increased moments of inertia resulted in less deflection.
4. Shear crack appeared near supports in strengthened beams, highlighting the negative effect of strengthening because of the rise of the load carrying ability.
5. Based on the recorded test results of concrete strain gauge, all tested beams exhibited ductile failure, where the reinforcing steel yielded before concrete crushing.
6. All strengthened beams failed with rupture, which is the most favorable failure mode, except for beam with 50 % RCA there was partial debonding of FRP.
7. Failure mode of the strengthened beams validates the effectiveness of the (EBROG) technique of strengthening.

References

[1] Jianzhuang Xiao, *Recycled Aggregate Concrete Structures*, Springer Berlin Heidelberg, pp. 65-68, 2017. [CrossRef] [Google Scholar] [Publisher Link]

[2] Mahir M. Hason, Mohamed H. Mussa, and Ahmed M. Abdulhadi, "Flexural Ductility Performance of Hybrid-Recycled Aggregate Reinforced Concrete T-Beam," *Materials Today: Proceedings*, vol. 46, pp. 682-688, 2021. [CrossRef] [Google Scholar] [Publisher Link]

[3] Hanaa Khaleel Alwan Al-Bayati et al., "Evaluation of Various Treatment Methods for Enhancing the Physical and Morphological Properties of Coarse Recycled Concrete Aggregate," *Construction and Building Materials*, vol. 112, pp. 284-298, 2016. [CrossRef] [Google Scholar] [Publisher Link]

[4] Mujaheed Yunusa et al., "Durability of Recycled Concrete Aggregates Prepared with Mechanochemical and Thermal Treatment," *Materials*, vol. 15, no. 16, pp. 1-14, 2022. [CrossRef] [Google Scholar] [Publisher Link]

[5] Ashtar S. Al-Luhybi, "Mechanical Properties of Recycled Aggregate Concrete with Steel Fiber: A Review," *Tikrit Journal of Engineering Sciences*, vol. 26, no. 3, pp. 37-42, 2019. [CrossRef] [Google Scholar] [Publisher Link]

[6] Nancy Kachouh et al., "Shear Behavior of Steel-Fiber-Reinforced Recycled Aggregate Concrete Deep Beams," *Buildings*, vol. 11, no. 9, pp. 1-19, 2021. [CrossRef] [Google Scholar] [Publisher Link]

[7] Kehan Chen et al., "Enhancement Treatment of Recycled Concrete Aggregate," *Frontiers in Built Environment*, vol. 7, pp. 1-3, 2021. [CrossRef] [Google Scholar] [Publisher Link]

[8] Wael Alnahhal, and Omar Aljidda, "Flexural Behavior of Basalt Fiber Reinforced Concrete Beams with Recycled Concrete Coarse Aggregates," *Construction and Building Materials*, vol. 169, pp. 165-178, 2018. [CrossRef] [Google Scholar] [Publisher Link]

[9] K. Ramadev, and R. Chitra, "Concrete Using Recycled Aggregates," *International Journal of Civil Engineering and Technology*, vol. 8, no. 9, pp. 413-419, 2017. [Google Scholar] [Publisher Link]

[10] Ali K. Khtara, Dr. Jamal, and A. Khudhair, "Flexural Behavior of Reinforced Concrete T-Beam Cast with Self-Compaction Concrete Incorporating Recycled Concrete Aggregate," *Muthanna Journal of Engineering and Technology*, vol. 6, no. 2, pp. 210-221, 2018. [CrossRef] [Google Scholar] [Publisher Link]

[11] Changyong Li et al., "Test and Evaluation of the Flexural Properties of Reinforced Concrete Beams with 100% Recycled Coarse Aggregate and Manufactured Sand," *Buildings*, vol. 11, no. 9, pp. 1-16, 2021. [CrossRef] [Google Scholar] [Publisher Link]

[12] Žarko Petrovic et al., "Experimental Analysis of Continuous Beams Made of Self-Compacting Concrete (Scc) Strengthened with Fiber Reinforced Polymer (Frp) Materials," *Applied Sciences*, vol. 11, no. 9, pp. 1-21, 2021. [CrossRef] [Google Scholar] [Publisher Link]

[13] Barbara Sadowska-Buraczewska, and Tomasz Chyzy, "Short Time Loads of T-Beams Made of Concrete Manufactured with the Use of High-Performance Recycled Aggregate," *IOP Conference Series: Materials Science and Engineering*, vol. 471, no. 5, pp. 1-13, 2019. [CrossRef] [Google Scholar] [Publisher Link]

[14] Abdullah M. Sagheer, Sami W. Tabsh, and Sherif Yehia, "The Structural Behavior of Reinforced Concrete Beams Made with Locally Produced Recycled Aggregate in the UAE," *Buildings*, vol. 13, no. 10, pp. 1-30, 2023. [CrossRef] [Google Scholar] [Publisher Link]

[15] Sindy Seara-Paz et al., "Flexural Performance of Reinforced Concrete Beams made with Recycled Concrete Coarse Aggregate," *Engineering Structures*, vol. 156, pp. 32-45, 2018. [CrossRef] [Google Scholar] [Publisher Link]

[16] In-Hwan Yang et al., "Structural Behavior of Concrete Beams Containing Recycled Coarse Aggregates under Flexure," *Advances in Materials Science and Engineering*, vol. 2020, no. 1, pp. 1-15, 2020. [CrossRef] [Google Scholar] [Publisher Link]

[17] Haider M. Abdulhusain, and Murtada A. Ismael, "Structural Behavior of Hollow Reinforced Concrete Beams: A Review," *Diyala Journal of Engineering Sciences*, vol. 13, no. 4, pp. 91-101, 2020. [CrossRef] [Google Scholar] [Publisher Link]

[18] Ahmmad A. Abbass et al., "Flexural Response of Hollow High Strength Concrete Beams Considering Different Size Reductions," *Structures*, vol. 23, pp. 69-86, 2020. [CrossRef] [Google Scholar] [Publisher Link]

[19] Haider M. Abdulhusain, and Murtada A. Ismael, "Flexural Behaviour of Hollow Reinforced Concrete T-Beams," *IOP Conference Series: Materials Science and Engineering: 1st International Conference on Engineering Science and Technology*, Samawah, Iraq, vol. 1090, pp. 1-11, 2021. [CrossRef] [Google Scholar] [Publisher Link]

[20] Mazin B. Abdulrahman, and Saba Muayad Mahmood, "Strength of Reinforced Reactive Powder Concrete Hollow Beams," *Tikrit Journal of Engineering Sciences*, vol. 26, no. 2, pp. 15-22, 2019. [CrossRef] [Google Scholar] [Publisher Link]

[21] Yahia M. Al-Smadi, Nasser Al-Huthaifi, and Ayah A. Alkhawaldeh, "The Effect of Longitudinal Hole Shape and Size on the Flexural Behavior of RC Beams," *Results in Engineering*, vol. 16, pp. 1-12, 2022. [CrossRef] [Google Scholar] [Publisher Link]

[22] Zahraa Sermed Zuhdiy, and Ali Laftah Abbas, "Comparative Study of Structural Behaviour of Reinforced Concrete Box Girder with Different Numbers of Cells," *IOP Conference Series: Materials Science and Engineering: 2nd International Scientific Conference of Engineering Sciences*, Diyala, Iraq, vol. 1076, pp. 1-9, 2021. [CrossRef] [Google Scholar] [Publisher Link]

[23] Hwai-Chung Wu, and Christopher D. Eamon, *Strengthening of Concrete Structures Using Fiber Reinforced Polymers (FRP): Design, Construction and Practical Applications*, Woodhead Publishing, 2017. [Google Scholar] [Publisher Link]

[24] Muktar Nuhu Danraka, H. Mahir Mahmod, and Ojo-kupoluyi Job Oluwatosin, "Strengthening of Reinforced Concrete Beams using FRP Technique: A Review," *International Journal of Engineering Science and Computing*, vol. 7, no. 6, pp. 13199-13213, 2017. [Google Scholar]

[25] Basem O. Rageh et al., "Flexural Behavior of RC Beams Strengthened with GFRP Laminate and Retrofitting with Novelty of Adhesive Material," *Buildings*, vol. 12, no. 9, pp. 1-24, 2022. [CrossRef] [Google Scholar] [Publisher Link]

[26] Sadjad A. Hemzah, Wajde S. Alyhya, and Saif A. Hassan, "Experimental Investigation for Structural Behaviour of Self-Compacting Reinforced Concrete Hollow Beams with in-place Circular Openings Strengthened with CFRP Laminates," *Structures*, vol. 24, pp. 99-106, 2020. [CrossRef] [Google Scholar] [Publisher Link]

[27] Athasit Sirisonthi et al., "Structural Behavior of Large-Scale Hollow Section RC Beams and Strength Enhancement Using Carbon Fiber Reinforced Polymer (CFRP) Composites," *Polymers*, vol. 14, no. 1, pp. 1-22, 2021. [CrossRef] [Google Scholar] [Publisher Link]

[28] Yousry B.I. Shaheen, Boshra Eltaly, and Amany Henish, "Response of Reinforced Concrete Box Girders Strengthened with Composite Materials," *Research Square*, pp. 1-22, 2022. [CrossRef] [Google Scholar] [Publisher Link]

[29] T. Kavitha, N. Swathi, and Sk. Jain Saheb, "Experimental and Numerical Study on Behavior of Externally Bonded RC T-Beams using GFRP Composites," *International Journal of Advance Research, Ideas and Innovations in Technology*, vol. 3, no. 6, pp. 719-732, 2017. [Google Scholar] [Publisher Link]

[30] Hasan Ehssan Alobaidi, and Alaa Hussein Al-Zuhairi, "Structural Strengthening of Insufficiently Designed Reinforced Concrete T-Beams using CFRP Composites," *Civil Engineering Journal*, vol. 9, no. 8, pp. 1880-1896, 2023. [CrossRef] [Google Scholar] [Publisher Link]

[31] K. Mallikarjuna et al., "Employing Carbon Fiber Reinforced Polymer Composites toward the Flexural Strengthening of Reinforced Concrete T-Beams," *ACS Omega*, vol. 8, no. 21, pp. 18830-18838, 2023. [CrossRef] [Google Scholar] [Publisher Link]

[32] ACI Committee, *Building Code Requirements for Structural Concrete (ACI 318-19): Commentary on Building Code Requirements for Structural Concrete (ACI 318R-19)*, American Concrete Institute, pp. 1-628, 2019. [Google Scholar] [Publisher Link]

[33] Rafaa M. Abbasa, and Wesal A. Fadala, "Behavioral Investigation of Reinforced Concrete T-Beams with Distributed Reinforcement in the Tension Flange," *E3S Web of Conferences*, vol. 318, pp. 1-11, 2021. [CrossRef] [Google Scholar] [Publisher Link]

[34] Rafaa M. Abbas, and Wesal A. Fadala, "Numerical Investigation of the Flexure Behavior of Reinforced Concrete Spandrel Beams with Distributed Tension Reinforcement," *Journal of Engineering*, vol. 28, no. 3, pp. 14-31, 2022. [CrossRef] [Google Scholar] [Publisher Link]

[35] Ayssar Al-Khafaji, and Hani Salim, "Flexural Strengthening of RC Continuous T-Beams Using CFRP," *Fibers*, vol. 8, no. 6, pp. 1-18, 2020. [CrossRef] [Google Scholar] [Publisher Link]

[36] Yanuar Haryanto et al., "Negative Moment Region Flexural Strengthening System of RC T-Beams with Half-Embedded NSM FRP Rods: A Parametric Analytical Approach," *Journal of the Chinese Institute of Engineers*, vol. 44, no. 6, pp. 553-561, 2021. [CrossRef] [Google Scholar] [Publisher Link]

[37] Yanuar Haryanto et al., "Validating an Analytical Method to Predict Flexural Behavior of RC T-Beams Retrofitted with Bonded Steel Wire Ropes in the Negative Moment Region," *AIP Conference Proceedings*: *The 3rd International Conference on Engineering, Technology and Innovative Researches*, Purbalingga, Indonesia, vol. 2482, no. 1, 2023. [CrossRef] [Google Scholar] [Publisher Link]

[38] Lawrence C. Bank et al., "*FRP Strengthening of Beams Made with Recycled Concrete Aggregate*," Symposium Paper, vol. 322, pp. 9.1-9.14, 2018. [Google Scholar] [Publisher Link]

[39] Amera H. Ftnan, and Ragheed F. Makki, "Behavior of Recycled Aggregate Concrete Beams Strengthened with FRP," *Kufa Journal of Engineering*, vol. 13, no. 4, pp. 13-24, 2022. [CrossRef] [Google Scholar] [Publisher Link]

[40] Riyam J. Abed, Mohammed A. Mashrei, and Ali A. Sultan, "Evaluating Flexural Strength of RC Beams Strengthened by CFRP using Different Analytical Models," *Civil and Environmental Engineering*, vol. 17, no. 2, pp. 465-475, 2021. [CrossRef] [Google Scholar] [Publisher Link]

[41] Malak H. Dawood, and Ali K. AL-asadi, "Flexural Behavior of Reinforced Recycled Aggregate Concrete Beams Strengthened by CFRP," *2022 International Symposium on Multidisciplinary Studies and Innovative Technologies (ISMSIT)*, Ankara, Turkey, pp. 134-141, 2022. [CrossRef] [Google Scholar] [Publisher Link]

[42] Mohammed. A. Mashrei, Jamal. S. Makkia, and Ali A. Sultan, "Flexural Strengthening of Reinforced Concrete Beams Using Carbon Fiber Reinforced Polymer (CFRP) Sheets with Grooves," *Latin American Journal of Solids and Structures*, vol. 16, no. 4, pp. 1-13, 2019. [CrossRef] [Google Scholar] [Publisher Link]

[43] Davood Mostofinejad, Seyed Masoud Shameli, and Ardalan Hosseini, "EBROG and EBRIG Methods for Strengthening of RC Beams by FRP Sheets," *European Journal of Environmental and Civil Engineering*, vol. 18, no. 6, pp. 652-688, 2014. [CrossRef] [Google Scholar] [Publisher Link]

[44] Hanan J. Qassim, and Mohammed A. Mashrei, "Flexural Strength of RC Continuous Beams Strengthened by CFRP Using EBR and EBROG Methods: Experimental and Analytical Study," *Civil and Environmental Engineering*, vol. 20, no. 1, pp. 580-592, 2024. [CrossRef] [Google Scholar] [Publisher Link]

[45] James K. Wight, and James G. MacGregor, *Reinforced Concrete: Mechanics and Design*, Pearson Education, pp. 1-1176, 2011. [Google Scholar] [Publisher Link]

[46] *BS 882:1992 Specification for Aggregates from Natural Sources for Concrete*, British Standard Institution, 1992. [CrossRef] [Google Scholar] [Publisher Link]

[47] IQS No. 5, Portland Cement, Iraqi Standard Specification, 2019. [Google Scholar] [Publisher Link]

[48] *ASTM A615/A615M-20 Standard Specification for Deformed and Plain Carbon-Steel Bars for Concrete Reinforcement*, ASTM International, pp. 1-8, 2018. [CrossRef] [Google Scholar] [Publisher Link]

[49] David Clayton Teychenné, R. E. Franklin, and Henry Chanoch Erntroy, *Design of Normal Concrete Mixes*, Department of the Environment, pp. 1-42, 1988. [Google Scholar] [Publisher Link]

[50] JJohn Newman, and B S Choo, *Advanced Concrete Technology 3: Processes*, Butterworth-Heinemann, 2003. [Google Scholar] [Publisher Link]

[51] *ACI PRC-440.2-17: Guide for the Design and Construction of Externally Bonded FRP Systems for Strengthening Concrete Structures*, American Concrete Institute, pp. 1-112, 2017. [Publisher Link]

[52] Adelino V. Lopes, Tiejiong Lou, and Sergio M.R. Lopes, "On the Ductility of RC Beam Section: A Revision and up to date of Conclusions," *Engineering Structures*, vol. 322, pp. 1-17, 2025. [CrossRef] [Google Scholar] [Publisher Link]

[53] *ASTM C1018-97 Standard Test Method for Flexural Toughness and First-Crack Strength of Fiber-Reinforced Concrete*, ASTM, International, 1997. [Publisher Link]

[54] Omar Fazaa Rajab et al., "Flexural Ductility, Stiffness, and Toughness of New Voided Reinforced Concrete One-Way Slab Using Waste Plastic Bottles," *Journal of Engineering*, vol. 2022, no. 1, pp. 1-10, 2022. [CrossRef] [Google Scholar] [Publisher Link]